Scopus

Documents

Summonte, C., Maccagnani, P., Desalvo, A., Bolognini, G., Ortolani, L., Sanmartin, M., Capelli, R., Bertoldo, M., Dinelli, F.

Gold nanoparticles on sodium alginate simulation of optical properties
(2018) *IET Conference Publications*, 2018 (CP748), .

2-s2.0-85065735843
Document Type: Conference Paper
Publication Stage: Final
Source: Scopus

GOLD NANOPARTICLES ON SODIUM ALGINATE: SIMULATION OF OPTICAL PROPERTIES

C. Summonte[1], P. Maccagnani[1], A. Desalvo[1], G. Bolognini[1], L. Ortolani[1], M. Sanmartin[1], R. Capelli[2], M. Bertoldo[3], F. Dinelli[4]

1 CNR-IMM UOS di Bologna, via Gobetti 101, 40126 Bologna, Italy
2 CNR-IOM s.s. 14, Km. 163.5 in AREA Science Park, 34149 Basovizza, Trieste, Italy
3 CNR-IPCF UOS di Pisa, via G. Moruzzi, 56124 Pisa- Italy
4 CNR-INO, Pisa - S. Cataldo, via Moruzzi,1 I-56124 Pisa, Italy
*summonte@bo.imm.cnr.it

Keywords: Gold nanoparticles, spectrophotometry

Abstract

UV-visible spectrophotometric properties of gold nanoparticles fabricated by magnetron sputtering on free-standing sodium alginate (SA) membranes have been recorded and simulated. The simulation implied the tuning of the collision frequency as well as the introduction of the Local Surface Plasmon (LSP) resonance in optical constants of the nanostructured material, which are based on a Drude-Lorentz model. The nanostructured film is treated by means of the Effective Medium Approximation. The film stack is simulated using the Generalized Transfer Matrix Method. The results show that the actual material can properly be treated, and quantitative results are obtained. A red shift in the LSP spectral position is observed for more interconnected material.

1. Introduction

Althought the simulation of optical properties of gold nanoparticles is being investigated since long [1], quantitative simulation of practical optical spectra obtained at laboratory level is subject to limitations mainly dictated by the non-ideality of real samples, and in particular homogeneity in size and shape of material agglomerates, or the presence of non-ideal substrates, which can be partially absorbing of not optically smooth, yet intriguing for special applications.
In this paper we report on the simulation of sphere-integrated UV-visible reflectance (*R*) and transmittance (*T*) of a set of self-organized gold thin films deposited by magnetron sputtering on free-standing membranes of sodium alginate (SA), which is a material with interesting properties for biomedical applications. The simulation model accounts for the following features, which vary from sample to sample: optical constant of gold thin films, which differs from the bulk case due to the limited mean free path of carriers; absorption signal due to the Localized Surface Plasmon (LSP) resonance; coverage of the substrate and presence of voids. The aim is to investigate the capabilities of the technique if applied to such non homogeneous films on non-ideal (partially absorbing; not opticall flat) substrate.

2. Experimentals

Free standing sodium alginate membranes were prepared by solution casting from 2 % wt Alginic Acid Sodium Salt (Sigma-Aldrich) solution in water. Each film was obtained from 8 ml of solution that was poured in a 5.5 cm Petri dish and left to dry at room temperature up to constant weight. The thickness of membranes, determined by simulation of the period of the interference pattern, spanned from 14 to 24 micron. Gold nanostructured films were deposited by magnetron sputtering at room temperature, using either 20 or 30 W Ar plasma power, with deposition time varying from 45 to 120 s. The deposition conditions are reported in Table 1. Scanning Electron Microscopy (SEM) images were obtained using a Zeiss CrossBeam340 equipped with InLens and ETH secondary electrons detectors. *R&T* spectra were obtained by means of an Avantes fiber optics UV-visible spectrophotometer (250-1100 nm spectral range) equipped with an integrating sphere. The simulations of *R&T* spectra were obtained using the computer code *Optical*, [2] based on the Generalized Transfer Matrix Method [3]. The optical model includes the SA membrane with finite thickness, and the nanostructured gold layer. The optical constants of SA were determined on uncovered membranes of varying thickness. Substrates of different thicknesses were used to separate the effect of absorption from that of surface roughness, both causing a decrease of the T signal.

Table 1 – Ar plasma power and deposition time of magnetron-sputtered Au films on SA.

	samples						
	G1	G2	G3	G4	G5	G6	G7
P (W)	20	30	20	20	20	30	30
t (s)	45	45	75	90	120	75	90

3. Results

Fig. 1 reports a sequence of SEM images taken on selected samples. The overall deposited material increases from left to right. Fig. 1-G1 shows the presence of only partially connected gold nanoparticles, about 60 nm diameter.

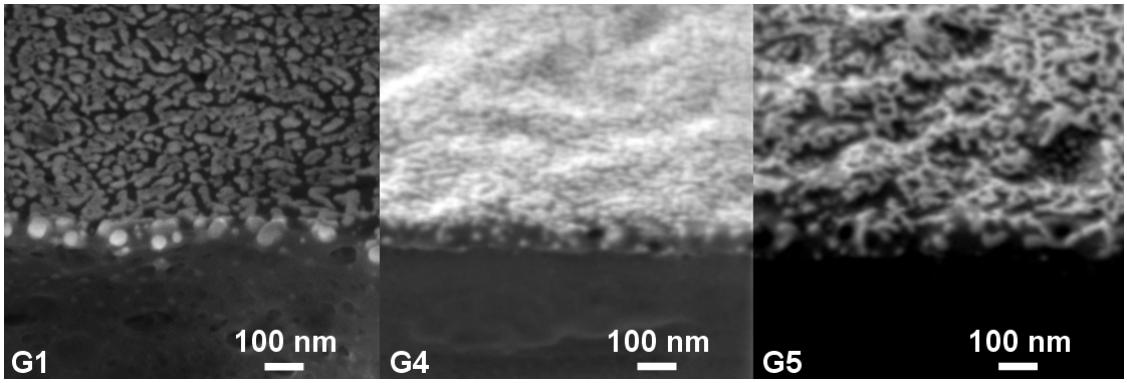

Fig. 1 SEM images of selected gold/SA films. The figures are labelled with the sample names. The scale is the same for all samples. The overall deposited material increases from left to right.

For increasing deposited material (Fig.1-G4, -G5), the substrate coverage increases, yet, the film remains nanostructured, showing the presence of an articulated patterns of voids.

Fig. 2. reports the experimental *R* and *T* spectra of all samples, as well as that of an uncovered SA membrane. The arrows indicate the direction of increase of the overall deposited material.

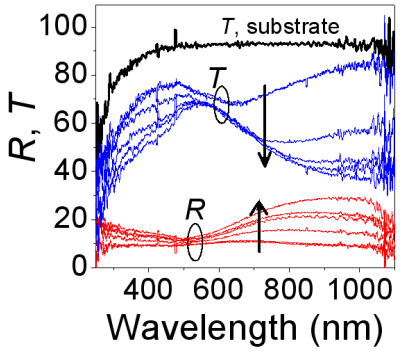

Fig. 2 Sphere-integrated *R* (red) and *T* (blue) of a set of gold films on SA, and *T* of a 14 μ SA membrane. The arrows indicate the direction of increase of deposited material.

Such spectra cannot be simulated using the optical constants of bulk gold. The reason is the presence of a maximum of *R* and a minimum of *T* in the red side of the spectrum (650-900 nm), which is incompatible with the monotonical increase of the extinction coefficient *k* of bulk gold in this region of the spectrum (see Fig. 3 below), due to free carrier absorption (FCA). To achieve a correct simulation, the free carrier contribution to the dielectic constant of the material must then be modutated, to account for the reduced mean free path L_f in the nanostructured material. However, the contribution of bound electrons, and therefore the plasma frequency, are not expected to vary. Going back to the observed minima/maxima, their existance is due to the presence of an absorption band with varying central energy, breadth, and amplitude. Such peak is attributed to the LSP resonance, similar to what proposed in Ref. [4] for the case of an ordered matrix of metal nanoparticles. The combined contribution of a variety of different shape or size is expected in our case.

Given such a picture, the optical constants of nanostructured gold have been simulated using an model that includes the sum of four Lorentz oscillators combined with the Drude FCA term (Refs. [5-7]]), where:

-a) Oscillator 1, 2 and 3 are mutuated from those of bulk gold. Oscillator 2 and 3 describe the electronic structure whereas Oscillator 1, out of range in the UV, mimics the dielectric constant at high energy.

-b) Of the two FCA parameters, the plasma frequency of bulk gold is maintained, whereas the collision frequency is left free in the simulation. The idea of separating the components of bulk gold optical constants to account for nanoparticle features is somewhat similar to what proposed by Haiss *et al.* (Ref.[8]).

-c) An additional oscillator is introduced to account for the LSP. The four parameters of such oscillator (enery, amplitude, broadening, energy dependent broadening parameter) are left free in the simulation.

The equation for the imaginary part of the dielectric constant of the nanostructured material is therefore given by:

$$\varepsilon_2(E)=\left(\sum_i \frac{\left((A_i-1)\cdot {E_{0i}}^2\right)\cdot \Gamma_{Bi}\cdot E}{\left(E_{0i}^2-E^2\right)^2+\left(\Gamma_{Bi}\cdot E\right)^2}\right)+\frac{{E_P}^2 E_T}{E\cdot(E^2+{E_T}^2)} \qquad (1)$$

The first term on the right in Eq. (1) is the sum of the four Lorentz oscillators, whereas the second term is the FCA contribution. A_i, E_i, Γ_{Bi} are the amplitude, energy, and broadening of oscillator *i*. *E* is the photon energy. The energy dependent broadening parameter Γ_{Bi} is given by:

$$\Gamma_{Bi}=\Gamma_i\cdot e^{-\alpha_i\cdot\left(\frac{E-E_{0i}}{\Gamma_i}\right)^2} \qquad (2)$$

where α_i is the Gaussian broadening parameter of oscillator *i* [5] [6]. E_P and E_T are the plasma frequency of bulk gold, and the collision frequency, both expressed in energy units, eV. The collision frequency is related to the mean free path L_f by:

$$E_T = \frac{\hbar \cdot v_F}{L_f} \qquad (3)$$

where v_F is the Fermi velocity for gold. The real part of the dielectric constant is numerically obtained by Kramers-Kronig transformation of ε_2:

$$\varepsilon_1(E) = 1 + \frac{2}{\pi}(C.P.)\int_0^{\infty} \frac{\omega \cdot \varepsilon_2(\omega)}{\omega^2 - E^2} d\omega \qquad (4)$$

where C.P. is the Cauchy principal value of the integral. Details on the formulations used in this paper and on the reason for the need of an energy-dependent broadening parameter can be found in Ref.[7]. All calculations were performed using the code *GTB-fit* [9]

We started by simulating the optical constant of gold given in Ref. [10] using Eq. (1) and (4). The result is reported in Fig. 3. The obtained parameters are reported in Table 2.

Table 2. Amplitude, energy, broadening, and energy dependend broadening parameter of Lorentz oscillators for bulk gold, obtained using Eq.(1) and (4). Moreover, E_P = 8.61±0.01eV; E_T = 60±3 meV

Oscillator	*A*	*E (eV)*	*Γ (eV)*	*α*
1	4.11±0.04	7.80±0.01	5.12±0.01	0.00*
2	3.10	3.99	1.93	1.40±0.05
3	1.90	2.86	0.87	1.96

*left fixed in the simulation

Based on SEM observations (Fig.1), the gold film is assumed to be mixed with voids and treated using the Bruggeman Effective Medium Approximation. The void fraction was fixed to 50% in order to limit the number of free parameters. Although this impacts on the obtained results, as film thickness is well below the onset of any interference pattern, misestimation of the void fraction merely tranfers on the determined thickness in the opposite direction. The simulations for samples G1, G4, and G5 are reported in figure 4. The figure shows that the model is appropriate to simulate

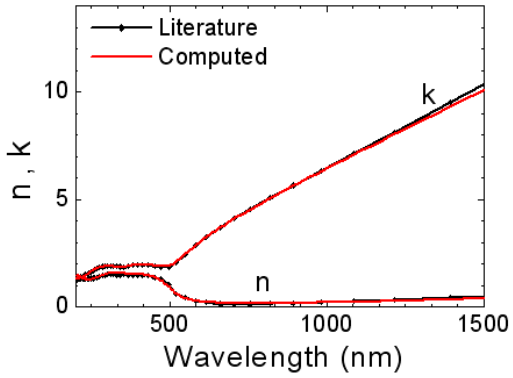

Fig. 3 Refractive index (*n*) and extinction coefficient (*k*) of bulk gold. Symbols: data from Ref. [10]. Line: fitting derived from the dielectric constants obtained using Eq.(1).

all experimental features, and in particular, the redshift of the maximum (minumum) of R(T) for increasing overall deposited material.

Table 3 reports the parameters obtained by the simulation. In Fig. 5 the contribution of the LSP oscillator to the imaginary part of the dielectric constant is reported. From the thickness obtained by the simulation, the deposition rate can also be determined. (Fig.6), which is 0.114 nm/s, provided the correctness of the choice of the 50% surface coverage. The result can be used in the calibration of the deposition instrument.

Table 3 – Parameters retrieved from the simulation.

	G1	G4	G5
Thickness, Gold* (nm)	5.5±1.0	9±2	14.±3
Thickness, SA (μm)	17±2	24±3	15±2
LSP Oscillator:			
A	11.4±4	22±7	19±6
E (eV)	1.88±0.01	1.47±0.01	1.39±0.01
Γ (eV)	0.84±0.01	0.80±0.01	0.65±0.01
α	1.84±0.05	2.00±0.05	0.850.05
E_T (eV)	≥ 250	≥ 3.3	≥ 9.6

* 50% alloyed with voids

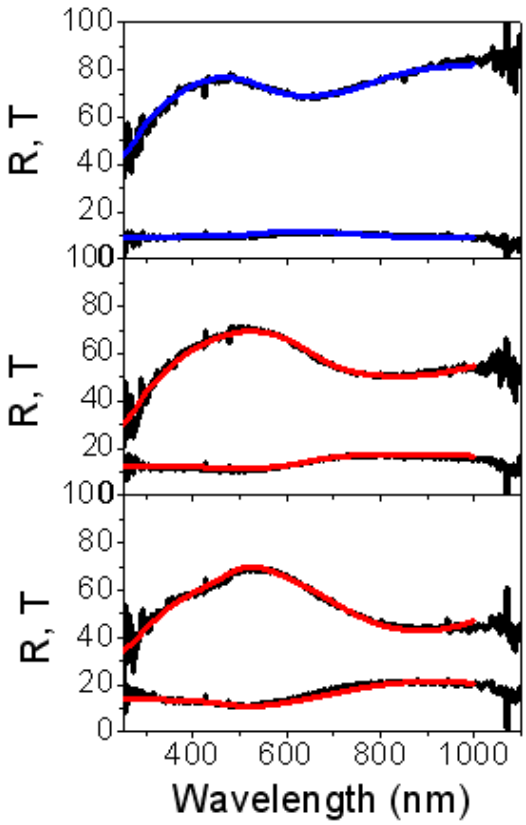

Fig. 4 Measured (black) and simulated (color) R&T spectra of (from top to bottom) G1, G4, and G5 samples.

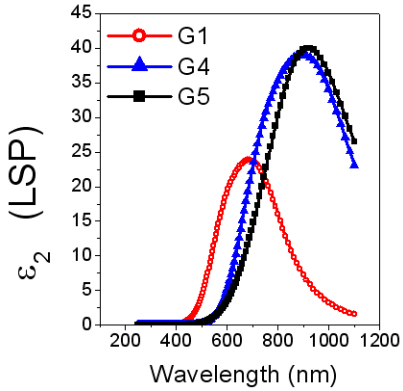

Fig. 5 LSP contribution to the imaginary part of the dielectric constant.

4. Discussion

We have shown that R&T spectra taken on thin and inhomogeneous gold films deposited on a practical substrate can be succesfully simulated, provided that the simulation takes into account the presence of LSP resonance. The increase of the collision frequency in the nanostructured material must also be taken into account. Moreover, the absorption band ascribed to the LSP resonance (Fig. 5), peaked at 660 nm for sample G1, shows a red shift for the remaining samples, being located at wavelengths longer than 800 nm. The feature is to be put in relation with the different

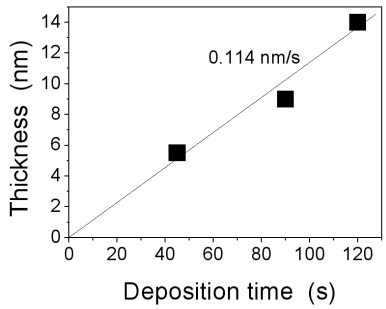

Fig.6 Film thickness as a function of deposition time

morphology of sample G1, which shows fairly isolated nanoparticles, compared to the coalescence observed.for the remaining samples. The noticeable spectral broadening of the LPS oscillator indicates a dispersion in the dimensions as well as on the shape of surface features affecting the propagation of surface modes.

However, a strong correlation between some of the retrieved parameters emerged from the analysis. Increasing film thickness, collision frequency, and SA substrate thickness, all result in a decrease of T in the blue end of the spectrum (wavelengths shorter than 500 nm), that is, a region not affected by the presence of the LSP. If the gold film thickness is underestimated, the amplitude of the LSP oscillator will be proportionally overestimated. This is the origin of the large error bars for the amplitude of the SA oscillator and film thickness (Table 2). However, other features such as the spectral resonant position of the LSP, as well as the broadening parameter, are not affected by such uncertainty and are correctly determined.

The strong parameter correlation is the reason why a more detailed descripiton, including, say, a mixed gold-SA phase, was not attempted.

5. Conclusions

Simulation of experimental sphere-integrated spectral reflectance and transmittance of gold nanoparticles on sodium alginate substrate is presented, based of Generalized Transfer Matrix Method. The optical constants of the nanostructured material are described using the Lorentz-Drude approach. The LSP is described by means of a specific oscillator, whereas the increased collision frequency with respect to bulk gold is accounted for by leaving as a free parameter the corresponding term .

Quantitative description of sample feature is achieved, and rapid, routine sample characterization can be exploited – however, the approach requires careful attention on the correlation of all parameters.

References

[1] Craig F. Bohren, Donald R. Huffman. Absorption and Scattering of Light by Small Particles, Wiley-VCH Verlag GmbH, 2007, DOI: 10.1002/9783527618156

[2] https://www.bo.imm.cnr.it/users/centurioni/optical.html

[3] E. Centurioni, Generalized matrix method for calculation of internal light energy flux in mixed coherent and incoherent multilayers, Appl. Opt. 44 (2005) 7532-7539

[4] D. Sikdar & A.A. Kornyshev, Theory of tailorable optical response of two-dimensional arrays of plasmonic nanoparticles at dielectric interfaces, Sci. Rep. 6, 33712; doi: 10.1038/srep33712 (2016).

[5] A. B. Djurišić, E. H. Li, Applied Optics 37 (1998) 5291

[6] A.D. Rakić, M. L. Majewski, J. Appl. Phys. 80 (1996) 5909

[7] C. Summonte, M. Allegrezza, M. Canino, M Bellettato and A. Desalvo, Analytical Expression for the Imaginary Part of the Dielectric Constant of Microcrystalline Silicon, Res Appl. Mater. 1 (2013) 6-11, available at: http://www.bo.imm.cnr.it/users/summonte/Analytical/Analytical.pdf

[8] W. Haiss, N.T.K. Thanh, J. Aveyard, D.G. Fernig, Determination of Size and Concentration of Gold Nanoparticles from UV-Vis Spectra, Anal. Chem 79 (2007) 4215-421

[9]https://www.bo.imm.cnr.it/users/summonte/minuit/minuitfit.html

[10]. B. Johnson and R. W. Christy. Optical constants of the noble metals, *Phys. Rev. B* **6**, 4370-4379 (1972)